Published in final edited form as:
Neuroimage. 2015 January 15; 105: 53–66. doi:10.1016/j.neuroimage.2014.10.047.

A Comparative Analysis of Mouse and Human Medial Geniculate Nucleus Connectivity: A DTI and Anterograde Tracing Study

Orion P. Keifer Jr.[3,6], **David Gutman**[1], **Erin Hecht**[4], **Shella Keilholz**[2], and **Kerry J. Ressler**[3,5,6]

[1]Department of Biomedical Informatics, Emory University, Atlanta, GA

[2]Coulter Department of Biomedical Engineering, Emory University/Georgia Institute of Technology, Atlanta, Ga

[3]Department of Psychiatry and Behavioral Sciences, Emory University School of Medicine, Atlanta, GA

[4]Department of Anthropology, Emory University, Atlanta, GA

[5]Howard Hughes Medical Institute, Chevy Chase, MD

[6]Yerkes National Primate Research Center, Atlanta, GA

Abstract

Understanding the function and connectivity of thalamic nuclei is critical for understanding normal and pathological brain function. The medial geniculate nucleus (MGN) has been studied mostly in the context of auditory processing and its connection to the auditory cortex. However, there is a growing body of evidence that the MGN and surrounding associated areas ('MGN/S') have a diversity of projections including those to the globus pallidus, caudate/putamen, amygdala, hypothalamus, and thalamus. Concomitantly, pathways projecting to the medial geniculate include not only the inferior colliculus but also the auditory cortex, insula, cerebellum, and globus pallidus. Here we expand our understanding of the connectivity of the MGN/S by using comparative diffusion weighted imaging with probabilistic tractography in both human and mouse brains (most previous work was in rats). In doing so, we provide the first report that attempts to match probabilistic tractography results between human and mice. Additionally, we provide anterograde tracing results for the mouse brain, which corroborate the probabilistic tractography findings. Overall, the study provides evidence for the homology of MGN/S patterns of connectivity across species for understanding translational approaches to thalamic connectivity and function. Further, it points to the utility of DTI in both human studies and small animal

Corresponding Author: Kerry Ressler, MD, PhD, Professor, Psychiatry and Behavioral Sciences, Yerkes Research Center, Emory University, 954 Gatewood Rd NE, Atlanta, GA 30329, off: 404-727-7739, kressle@emory.edu.

Conflicts of Interest: The authors declare no conflicts of interest.

modeling, and it suggests potential roles of these connections in human cognition, behavior, and disease.

Keywords

Medial Geniculate Nucleus; Diffusion Tensor Imaging; Diffusion Weighted Imaging; Magnetic Resonance Imaging; Tractography; Connectome

1. Introduction

The thalamic nuclei are critical for interfacing and organizing cortical and subcortical connectivity and functioning. Traditionally, thalamic nuclei like the medial and lateral geniculate have been described as relay stations for auditory and visual information, respectively. For example, the most studied function of the medial geniculate nucleus (MGN) is its role in passing auditory information from the inferior colliculus to the auditory cortex (Budinger et al., 2000; Crippa et al., 2010; Geiser et al., 2012; Horie et al., 2013; Jones, 1985; Llano and Sherman, 2008; Mesulam and Pandya, 1973; Monakow, 1914; Poliak, 1926; Redies et al., 1989; Ryugo and Killackey, 1974; Tunturi, 1946; Walker, 1937). However, there is also evidence the MGN has a far broader role in multisensory processing (Blum et al., 1979; Brinkhus et al., 1979; Carstens and Yokota, 1980; Love and Scott, 1969; Wepsic, 1966). Further, there is growing evidence that the MGN does not operate in isolation from other posterior thalamic nuclei (i.e. the posterior intralaminar, suprageniculate, and peripeduncular nuclei) which are in very close proximity and may be part of a more collective functional system(Linke and Schwegler, 2000; Winer and Morest, 1983). In fact, there is preliminary evidence that the MGN and surrounding nuclei (here to referred to as ‘MGN/S’,) project to the amygdala (Carter and Fibiger, 1977; LeDoux et al., 1985a; LeDoux et al., 1985b; Ottersen and Ben-Ari, 1979; Shinonaga et al., 1994), insula/parainsular area (Clasca et al., 1997; Guldin and Markowitsch, 1984; Linke and Schwegler, 2000), caudate/putamen(LeDoux et al., 1985a), globus pallidus(Moriizumi and Hattori, 1992), the hypothalamus(LeDoux et al., 1985a; LeDoux et al., 1984), the thalamus(LeDoux et al., 1985a; LeDoux et al., 1984), and the midbrain(Moriizumi and Hattori, 1992). Additionally, the MGN/S receives input from the globus pallidus(Shammah-Lagnado et al., 1996), the auditory cortex(Roger and Arnault, 1989) (Winer et al., 2001), the insula(Cranford et al., 1976), the cerebellum(Raffaele et al., 1969) (Zimny et al., 1981), and the inferior colliculus(Benevento and Fallon, 1975).

Since the MGN/S plays a central role in sensory processing, a thorough understanding of its anatomy and function are important for understanding certain disorders. For example, the function of the MGN/S has been well-established in auditory fear learning (LeDoux et al., 1985a; LeDoux et al., 1985b, 1986; LeDoux et al., 1984). Further, recent studies have suggested that thalamic auditory processing may play a role in tinnitus(Aldhafeeri et al., 2012; Crippa et al., 2010; Landgrebe et al., 2009; Muhlau et al., 2006; Su et al., 2012), attention deficit disorder(Hart et al., 2013; Schweitzer et al., 2004; Xia et al., 2012), and schizophrenia(Dorph-Petersen et al., 2009; Smith et al., 2011). However, the broad network connectivity of the MGN/S is not currently well-established nor is the role of these connections. Further, the majority of the cited work above has focused on the rat model.

Given that the mouse model offers opportunities for neuro-genetics research and work in human patient populations can directly address the role of the MGN/S in disease studies, studying both is imperative to future progress.

Unfortunately, there is a paucity of studies addressing these issues. Furthermore, existing MGN/S connectivity work uses different methodologies in mice versus humans - mouse MGN/S connections were studied using injection tract tracing(Horie et al., 2013; Llano and Sherman, 2008), while human MGN/S connections to the amygdala and the inferior colliculus used diffusion weighted MRI methods(DTI)(Crippa et al., 2010; Devlin et al., 2006; Javad et al., 2013). Furthermore, given that anatomy and physiology differ in some systems between humans and other species (Carlson, 2012; Manger et al., 2008; Preuss, 2000; Smulders, 2009), verification of homologous MGN/S connectivity across species is an important foundational step for translational research.

Here we present a whole-brain exploration and comparison of the general patterns of connectivity of the mouse and human MGN/S probabilistic tractography. Further, we focus down on the specific patterns of connectivity between the MGN/S and the amygdala, auditory cortex, and fastigial nucleus of the cerebellum to explicitly compare between humans and mice. These analyses and comparisons are important because probabilistic tractography is often cited as a translationally useful tool (and a powerful comparative anatomy tool between humans and other primates (Hecht et al., 2013; Rilling et al., 2008; Thiebaut de Schotten et al., 2012; Zhang et al., 2012), but there is a dearth of studies linking small animal models (e.g. mouse) to humans. Therefore, the objectives of the following paper are to address the broad patterns of connectivity as predicted by probabilistic tractography of the human and mouse MGN/S, to provide evidence for the comparative utility of probabilistic tractography by focusing on the specific patterns of connectivity between species, and to partially validate the results of small animal probabilistic results with anterograde tracing from the MGN/S. First, we hypothesized that humans and mice would show connectivity patterns between MGN/S and the amygdala, auditory cortex, caudate/putamen, globus pallidus, thalamus, hypothalamus, cerebellum, and insula. Additionally, we sought to further validate(Gutman et al., 2012) the mouse probabilistic tractography results by comparing them to anterograde tracing results in the MGN/S. We hypothesized that the mouse probabilistic tractography results would recapitulate the patterns of connectivity evaluated using anterograde tracing.

2. Materials & Methods

2.1 Human Participants

All study procedures were approved by the institutional review board of Emory University. A total of 10 African American women and 3 African American men, aged 20–52 (mean age of 38 years old) were recruited under a broader, on-going neuroimaging study of risk factors for PTSD in civilians(Fani et al., 2013; Fani et al., 2012). The participants selected for the current student were randomly sampled from the control arm of the study. All participants underwent a screening procedure to ensure there was no active use of psychotropic medication, no current alcohol or substance abuse, no history of psychiatric

disorders, no history of head injury or other neurological disorders. All female participants received a pregnancy test prior to the imaging session.

2.2 Animal Studies

2.2.1 MRI Arm—All imaging was conducted on naive 8 week old C57BL/6J male mice (n=10). The 10 mice were placed under anesthesia using ketamine/ dexmedetomidine, were perfused with 10 mls phosphate buffered saline (PBS, PH 7.4), followed by 10 mls 4% paraformaldehyde (PF) in PBS and then postfixed (for 24 hours) in the same 4% PF/PBS. The brains were then embedded in an agarose-gadolinium (III) oxide matrix for imaging. Previous work has shown the validity and utility of using this method (Gutman et al., 2012).

2.2.2 Anterograde Biotinylated Dextran Amine (BDA) Tracing Arm—A separate cohort of naive 8week old C57BL/6J male mice (n=5, Jackson Labs, Bar Harbor, Maine) were used for the anterograde tracing (using 10,000 MW, BDA) arm of the study. The details of the BDA method are presented elsewhere (Gutman et al., 2012), but in brief, injections of 0.15 microliters of BDA were targeted at the MGN/S (−3.0mm AP, +/− 2.2 mm ML, − 3.2 mm DV from Bregma) using a Stoelting *Just for Mice* Stereotax (Wood Dale, Illinois) with a Hamilton Neuros 5 microliter syringe driven by a World Precision Instruments UMC4-J pump controller and UMP3 pump (Sarasota, Fl). The duration of injection was 1 minute with the syringe left in place for 10 minutes followed by syringe withdrawal over the course of 1 minute. The mice were perfused 1 week later, their brains extracted, sectioned (35 microns), mounted, and examined on a Nikon E800 microscope with a Darklite Illuminator (MVI, Inc, Avon, MA).

2.3 Magnetic Resonance Imaging - Human

All human MRI scanning was conducted on a research-dedicated Siemens 3-Tesla TIM-Trio Scanner (Munich, Germany) that is part of the Emory/Georgia Tech Biomedical Imaging Technology Core (BITC). The parameters used for the diffusion weighted imaging scans are found in previous work(Fani et al., 2012). In brief, the slice thickness was 2mm, with an imaging matrix of 128 x 128, and a field of view of 256 mm x 256 mm, TE = 154 ms, TR 13500 ms, and b = 1000 s/mm^2. There were 60 diffusion weighted volumes with 3 b0 volumes. Additionally, T1 anatomical scans were acquired with an MPRAGE sequence with a slice thickness of 1mm, imaging matrix 256 x 256, FOV = 256 mm x 256 mm, TE = 3.02 ms and TR = 2600 ms.

2.4 Magnetic Resonance Imaging – Mouse

All mouse MRI scanning was conducted on a research dedicated Bruker 9.4 Tesla MRI scanner (Billerica, MA). All brains were scanned using our previously designed *ex vivo* procedure(Gutman et al., 2012; Gutman et al., 2013). In brief, perfused mouse brains were embedded in a gadolinium agarose matrix and scanned at multiples of 6 with a T2 RARE sequence and a 60 direction DWI sequence. T2-weighted images were first acquired at 161 micron isotropic resolution (TE = 26ms, matrix 256 x 512, 20 averages, scan time ~ 16 hours). Diffusion weighted images were then acquired using a 2-D spin-echo based sequence with 200 micron isotropic resolution. (TE = 26.9 ms, TR=10000 ms, matrix size of

256 x 128, 60 axial slices collected/tube, 60 gradient directions with a diffusion weighting b=2000 s/mm^2, and 3 b0 images).

2.5 Seed Generation

All post-acquisition processing was conducted as analogously as possible between the human and mouse data sets (differences in processing are noted). Since the mouse volumes were collected 6 at a time, each mouse volume was isolated from the larger raw imaging volume as previously described(Gutman et al., 2012). From there, the human and mouse diffusion volumes were processed by isolating them either from the skull (human) or the embedding matrix (mouse), using the Brain Extraction Toolkit (BET(Smith, 2002), http://fsl.fmrib.ox.ac.uk/fsl/fslwiki/BET). Both human and mouse brains were then processed using the FSL DTI pipeline in preparation for probabilistic tractography (FDT)(Behrens et al., 2007; Behrens et al., 2003), http://fsl.fmrib.ox.ac.uk/fsl/fslwiki/FDT).

The MGN/S seeds were based on anatomical localization with the use of the Atlas of the Human Brain (with guidance from (Devlin et al., 2006)) and the Paul Allen mouse reference atlas (Lein et al., 2007). Given the higher resolution, all seeds were defined in anatomical space, to which the b0 images, and consequentially probabilistic tractography results, were registered for evaluation. In particular, after the initial placement of the MGN/S seed based on anatomy in the high resolution anatomical scan, it was then was cross referenced with tractography results from seeds placed within the auditory cortex and inferior colliculus (Figure 1). For example, with the human MGN/S regions of interest (ROIs), they were drawn in the T1 weighted high resolution space (e.g. the MGN/S is ventral to the ventral posterolateral thalamic nucleus and anterior pulvinar nucleus, dorsal to the cerebral peduncle, medial to the lateral geniculate, and lateral to the dorsal trigemino-thalamic tract), which was then overlaid with back-transformed probabilistic connectivity maps of the auditory cortex (AC) and inferior colliculus(IC). The anatomically defined MGN/s seed was constrained to the area covered by the projections from the AC and IC. Further, the tracts from the visual cortex were also generated and used to ensure that the MGN/S was isolated from the lateral geniculate nucleus (i.e. no portion of the MGN/S seed overlapped with the areas covered by the tracts from the visual cortex). The mouse MGN/S seeds were analogously generated and checked, though their anatomical identification is significantly easier given the anterior to posterior displacement of the nuclei (e.g. posterior to the LGN, medial to the hippocampus, lateral to the midbrain).

2.6 General Probabilistic Tractography Analysis

Probabilistic tractography, with multi-fiber reconstruction (probtrackx), was then generated for each voxel within the MGN/S seed mask (all default settings were used except for the inclusion of Euler streamlining and distance correction). *A priori* exclusion masks were placed in the occipital lobe and pre/postcentral gyrus to help mitigate spurious tractography results from the lateral geniculate and ventrolateral nuclei which are located adjacent to the medial geniculate. Further, exclusion masks were placed at the natural boundaries in the brain including the ventricles (mouse and humans) and the interface between the hippocampus and the midbrain/thalamus (mouse, to prevent tractography errors due to partial voluming effects in this area). Using a standard two-level registration process, the

probabilistic tractography results were transformed (using the inverse matrix of registering the lower resolution b0 image to the higher resolution anatomical scan) into each subject's high resolution mouse T2 or human T1 space. The individual subject's high resolution images were then registered to a common imaging space (e.g. Montreal Neurological Institutes 152 Brain 6th Generation(Grabner et al., 2006) for humans or our own standard mouse space template(Gutman et al., 2012; Gutman et al., 2013)). Placing the results in common space allows for better identification of anatomy and also facilitates group level analysis.

For a general analysis of the tract distributions with respect to the MGN/S, the tractography results were set to a threshold 0.1% of the maximum number of tracts in a subject (Devlin et al., 2006). These thresholded results were then either averaged across the group or binarized and summed. The use of binarization and summation of the results highlights how consistent a particular set of tracts were across subjects. The human results were submitted to FSL Atlasquery function to determine the areas of the brain were the MGN connectivity mapped onto the MNI152 space. The mouse results were compared to the Paul Allen Brain mouse reference atlas (Allen Institute for Brain Science, Allen Mouse Brain Atlas (Lein et al., 2007), http://mouse.brain-map.org/static/atlas) to determine areas of connectivity.

2.7 Focused Probabilistic Tractography Analysis

Since the general analysis of tract distributions is necessarily broad and difficult to parse into pathways of connectivity, the specific patterns of connectivity between the MGN/S and the amygdala, auditory cortex, and fastigial nucleus were analyzed for both the human and mouse data. In particular, seeds were generated for auditory cortex, amygdala and fastigial nucleus of the cerebellum, which were then used as "waypoint" masks when analyzing the probabilistic tractography of the MGN/S (i.e. the results would only show tracts starting at the MGN/S and passing through the waypoint). The same exclusion masks and probtrackx settings were used for this analysis, as were used for the general analysis. Unlike the general analysis, the threshold for these images was increased to 10% of the maximum projection since the analysis was constrained to the connectivity between two areas of the brain, meaning less overall spurious connections and hence less "noise".

3. Results

3.1 Isolation of Human MGN/S

The results presented in Figure 1 illustrate the anatomical localization of the medial geniculate in each human participant (panel A) based on the Mai, Paxinos and Voss Atlas of the Human Brain(Mai et al., 2008). As a form of validation for the accuracy of these seed placements, these localizations were cross referenced to projections from the inferior colliculus (panel B) and the primary auditory cortex. The visual cortex connectivity distribution was used to confirm the differentiation of the medial geniculate nucleus from the lateral geniculate nucleus (panel C). Each individual human brain (shown in a consistent position across figures on the surrounding border, with the male participants shown on the lower right three brains) showed the same pattern of the auditory cortex connecting more medially (shown in the red to yellow overlay) when compared to the visual cortex

projections which had more lateral projections (shown in the light to dark blue overlay). Importantly, all of the anatomically defined MGN/S seeds fell within the pathway of the inferior colliculus and auditory cortex and did not require modification.

3.2 General MGN/S Probabilistic Connectivity in Humans

Following MGN/S seed generation and isolation, the general connectivity of the human MGN/s was analyzed and the results are presented in Figure 2. The results (Figure 2, Panel A) highlight the human probabilistic connectivity between the MGN/S and the amygdala (highlighted in purple on the atlas image), caudate, putamen, and globus pallidus on the MNI152 2mm atlas at A-P slice 64 as compared to Plate 25 from the Human Brain Atlas(www.thehumanbrain.info, Dusseldorf, Germany). Moving more posteriorly to MNI slice 52, Panel B (middle Panel) details the connections between the MGN/S and the auditory cortex (highlighted in purple on the atlas image), middle temporal cortex, posterior putamen, insula, thalamus, and portions of the midbrain as compared to Plate 40 from the Human Brain Atlas. Moving most posteriorly to A-P slice 32, Panel C (bottom panel) shows the connectivity of the MGN/S and the cerebellum as compared to the cerebellar atlas standard in FSL atlas resources(Diedrichsen et al., 2009). The results are tabulated in the second column of Table 1 with the number of participants showing the pattern of connectivity. A few examples are worth highlighting with respect to the next few results sections. Looking to connectivity between the MGN/S and amygdala, it is notable that 13 of 13 subjects showed the connectivity on the right side, and 12 of 13 subjects showed the connectivity on the left side. Likewise, the connectivity between the MGN/S and the cerebellum had 13 of 13 subjects showing the connectivity on the left, and 11 of 13 subjects showing connectivity on the right. It is interesting to note, that despite the use of the auditory cortex probabilistic tractography as a means to confirm the location of the MGN/S, the patterns of connectivity between the MGN/S and the auditory cortex only showed 8/13 subjects for both hemispheres when using the 0.1% threshold and then binarizing. Further, it is worth noting that in the areas immediately adjacent to the MGN/S there is a diffuse pattern of connectivity throughout the thalamic regions.

3.3 MGN/S Probabilistic Connectivity in Mice

Paralleling the results found in humans, the results of the probabilistic connectivity of the MGN/S in mice are presented in Figure 3. In particular the surrounding border of each panel show the tractography results for each mouse thresholded at 0.1%. The left-center image shows the binarized and summated image of those results threshold at least 5 brains. Moving from anterior to posterior, panel A (top panel) highlights the connectivity of the MGN with the amygdala, caudate putamen, thalamus and hypothalamus as compared to section 70 of the Paul Allen Mouse Brain Reference Atlas (atlas.brain-map.org). In panel B, the connectivity maps show connections to the auditory cortex, thalamus, hypothalamus, and portions of the midbrain as compared to section 2 of the Paul Allen Brain atlas. Panel C shows the connections between the MGN and the cerebellum, particularly the fastigial nucleus as compared to section 116 of the Paul Allen Mouse Brain Reference Atlas. Looking at the same patterns noted in section 3.2 for humans, the mouse probabilistic tractography showed that 6/10 mice showed connections to the amygdala in both hemisphere. Likewise 9/10 mice showed connections to the auditory cortex in both

hemisphere. Finally, on the right hemisphere 8 of 10 mice and on the left hemisphere 9 of 10 mice showed connectivity between the MGN/S and fastigial nucleus of the cerebellum. Like in the human results, it is worth noting that in the areas adjacent to the MGN/S there is a diffuse pattern of connectivity throughout the thalamic regions and also the midbrain regions.

3.4 Focused Mouse Connectivity Comparisons in Midbrain and Thalamus

Given the rather diffuse tractography results when seeding the mouse MGN/S, it is important to evaluate the results with respect to the underlying axonal tracts. Therefore, Figure 4 compares the general probabilistic tractography results at different thresholds (1%, 10%, 25%, and 50%) to a matched brain section from the BDA anterograde tracing arm of the study. Figure 4A shows a zoomed in section focused on the thalamus and hypothalamus when compared to Section 73 and 74 of the Paul Allen Brain Atlas (not shown in Figure). Notably there are projections to the lateral posterior nucleus and central medial nucleus of the thalamus, the zona incerta of the hypothalamus, and the posterior hypothalamic nucleus. In addition to these areas that receive the MGN/S projections, it is notable that the 4A also shows extensive fibers of passage through the thalamus and hypothalamus (though the fibers are faint in the captured image) and fibers coursing through the medial lemniscal pathway and the internal capsule. Figure 4B shows a very stringently thresholded (50%) probabilistic tractography image which shows a strong concordance (see white arrows) with the areas of higher BDA density. Figure 4C–E highlights how reducing the threshold increases the distribution of tracts. It is worth noting, that while thresholds of 10% and above do appear to increase the concordance with the retrograde imaging overall, there is the loss of certain probabilistic tractography results like the auditory cortex which are apparent at 0.1% threshold (see discussion for further consideration).

3.5. Comparisons of Connectivity between the MGN/S and the Amygdala, Auditory Cortex, Fastigial Nucleus

In order to distinctly compare the patterns of connectivity of the MGN/S between humans and mice, a focused analysis of the patterns of probabilistic connectivity was conducted between the MGN/S and the amygdala, auditory cortex, and fastigial nucleus of the cerebellum in humans and mice. Figure 5 shows the results of the analysis for the connectivity between the MGN/S and the amygdala. Figure 5A shows the average tracts across the 13 human brains that exist between the MGN/S and the amygdala, with Figure 5B showing a more posterior section showing that the pathway of the tract is through the internal capsule. Likewise the left side of Figure 5C shows the patten of connectivity between the MGN/S and amygdala in the mouse, which also crosses through the internal capsule. The corresponding section with the anterograde BDA tracing shows that the tracts do pass from the MGN/S and course through the internal capsule before termination on the amygdala. Figure 5D shows an adjacent BDA anterograde section with the rather extensive coverage of the amygdala.

Likewise, Figure 6 shows the patterns of connectivity between the MGN/S and the auditory cortex as compared between humans and mice. Figure 6A shows the average tracts across the 13 human subjects between the MGN/S and the auditory cortex, with Figure 6B showing

their path through the internal capsule, particularly the posterior limb, which cross over the external capsule. These results are echoed in the mice in Figure 5C with left side of the image showing the probabilistic tractography results to the auditory cortex using the internal capsule, then crossing the external capsule with the concurrent anterograde tracing results showing the same pattern. Figure 5D shows the density of the anterograde tracing in an adjacent posterior section that covers the auditory cortex in a pattern consistent with Figure 3B.

Next, Figure 7 highlights the patterns of connectivity between the MGN/S and the fastigial nucleus of the cerebellum between humans and mice. Figure 7A shows the average tracts for the human subjects between the MGN/S and the fastigial nucleus of the cerebellum as determined using a previously published probabilistic atlas of the cerebellum(Diedrichsen et al., 2011). Looking at a sagittal perspective, the connectivity between the fastigial nucleus and the MGN/S is mediated by the superior cerebellar peduncle. These results are mirrored in the mouse probabilistic tractography data as well, Figure 7C showing the average tracts between the MGN/S and the fastigial nucleus as determined using the Section 116 of the Paul Allen Brain Mouse Atlas.

Finally, Figure 8 presents an overview of the anterograde tracing results used for comparison to the probabilistic tractography in mice. Of the five mice used for the study, one showed the most concordance with the MGN/S seed used for the mouse probabilistic tractography analysis. The results from the anterograde tracer injections for that mouse are detailed in Table 1 along with comparison to the results of the general connectivity patterns seen in Figure 3. In agreement with the mouse probabilistic tractography results there were fibers of passage and termination through the thalamus, hypothalamus, and midbrain. Additionally, there were dense projections that terminated in the auditory cortex, amygdala, and the caudate/putamen.

4. Discussion

Though the classical role of the MGN is to relay information to the auditory cortex, the numerous other projections from the MGN and surrounding areas need further exploration. This is particularly important since recent studies have suggested that thalamic auditory processing may play a role in tinnitus(Aldhafeeri et al., 2012; Crippa et al., 2010; Landgrebe et al., 2009; Muhlau et al., 2006; Su et al., 2012), attention deficit disorder(Hart et al., 2013; Schweitzer et al., 2004; Xia et al., 2012), and schizophrenia(Dorph-Petersen et al., 2009; Smith et al., 2011), though the exact circuits for these diseases has not been postulated. Here we have shown that the connections previously found in rats also exist in both humans and mice, which expanded our understanding of both mouse and human MGN/S connectivity over previous work. More pointedly, we have directly compared the connections between the MGN/S and the auditory cortex, amygdala, and the fastigial nucleus of the cerebellum, which showed distinct homology between humans and mice, and also corresponded to the anterograde tracing results presented here. Looking more broadly, these results suggest a common pattern of connectivity between mice, rats, and humans, suggesting that these connections are likely evolutionarily conserved throughout the mammalian family tree. Additionally, we have further expanded the corroboration of diffusion weighted MRI based

probabilistic tractography in mice with the use of the anterograde tracing molecules biotinylated dextran amine(Gutman et al., 2012).

Our comparison of the broad patterns of probabilistic tractography in mice and humans revealed connections between the MGN/S and the auditory cortex, amygdala, globus pallidus, caudate/putamen, hypothalamus, thalamus, and cerebellum. Interestingly, we also saw connections with the middle temporal cortex (discussed further below). A review of the literature reveals that the functional role of these specific connections is not apparent. Of the medial geniculate connections, the most studied is the reciprocal connection between the amygdala (central and lateral) and MGN. Early work by Ledoux and colleagues showed that the connection between the auditory thalamus and the amygdala, but not necessarily the auditory cortex to the amygdala, was important for auditory fear conditioning in the rat (LeDoux et al., 1984). Further exploration of the connections from the MGN provided evidence that disruptions of the MGN - amygdala tracts, but not to the caudate/putamen, resulted in diminished fear conditioning responses(Iwata et al., 1986; LeDoux et al., 1985a; LeDoux et al., 1986). However, whether this pathway serves a broader role in cognition and behavior is still unclear.

With regards to the connections with the caudate-putamen, our results are also consistent with past work in the rat(LeDoux et al., 1984; Ryugo and Killackey, 1974) that showed the primary source of these projections were the ventral and dorsal subdivisions of the MGN (Ryugo and Killackey, 1974). Beyond tract tracing, there is converging evidence for the connection in the form of evoked unit responses in striatal neurons when electrical stimulation is applied to the medial geniculate nucleus(Clugnet et al., 1990). With the pallidum there is evidence in the rat that there are reciprocal projections between the medial portion of the medial geniculate and the globus pallidus (Moriizumi and Hattori, 1992; Shammah-Lagnado et al., 1996). The role of the connection between the MGN and globus pallidus is unclear. Clearly there is a lack of research on the role of the direct connections between the MGN and the caudal portions of the caudate-putamen and globus pallidus. However, looking more broadly, there is accumulating evidence for the basal ganglia in processing auditory information, including projections from the auditory cortex(McGeorge and Faull, 1989). Such work is now coalescing into a broadly accepted theory that the basal ganglia is involved in temporal auditory perception (e.g. beat perception)(Grahn and Brett, 2007), in the synchronization of auditory and visual sensory information(Freeman et al., 2013), in the processing of language(Lieberman et al., 1990), and in vocal learning and perception in song birds(Hessler and Doupe, 1999) (Brainard and Doupe, 2000). Inputs from the MGN/s (and vice versa) into the basal ganglia may sub-serve important roles in these facets of cognition and behavior.

The connections between the hypothalamus and the MGN/S implicate a potential neuroendocrine role. Both the BDA tracing results and the probabilistic results suggest that there is a fair degree of connectivity between the MGN/S and the hypothalamus (albeit the BDA staining density is lower than seen in the other areas). Of the results presented here with humans and mice there is a match to previous work in rats showing a projection from the immediately adjacent area of the MGN to the ventromedial hypothalamus(LeDoux et al., 1984). A study of this connection has shown that lesions to the MGN, and potentially

surrounding nuclei, drastically reduce the release of corticosterone released in response to audiogenic stress (restraint and ether stress showed normal corticosterone release)(Campeau et al., 1997). Likewise our results that in humans and mice there are notable connections between the MGN/S and the zona incerta, which has been substantiated in rats (Power et al., 1999), though again the role of this connection is poorly understood.

Regarding the connectivity between the MGN/S and the rest of the thalamus, there is evidence that the immediately adjacent areas around the MGN/S send projections to the subparafasicular nucleus in rats (LeDoux et al., 1985a; LeDoux et al., 1984; Wang et al., 2006). We show the same connections using our classical tracing study in mice. Interestingly, very little is known about the subparafasicular nucleus, though it is known that it is the point of convergence of input from medial prefrontal, insular, and ectorhinal cortices, as well as the lateral septum, amygdala, portions of the hypothalamus, periaqueductal gray, and several other nuclei(Wang et al., 2006). Based on the source of these afferent inputs it has been postulated that the area is involved in reproductive, visceral, nociceptive, and auditory functions. Looking more broadly at Table 1 and the results in the Figure 2, 3, and 8, it would appear that there are numerous other connections between the MGN/S and thalamus that should be explored. Finally, focusing to the connectivity between the MGN/S and cerebellum, there is limited early work in the cat and the rat that substantiate these tracts, though little work has followed up to determine the role of the connection (Raffaele et al., 1969; Zimny et al., 1981)

Overall, the probabilistic tractography results show that there are large similarities in the broad patterns of connectivity between mice and humans (see Table 1). These similarities suggest that these connections have functional utility though these functions are still poorly understood. Interestingly, there are points of discordance in the comparison between the two species. The human data shows unilateral projections to the middle temporal cortex, which does not have direct connectivity to MGN or adjacent nuclei. Further analysis will be necessary to determine whether these unknown connections are a false positive result of probabilistic tractography algorithm. Further, the human data showed connectivity between the MGN/S and the insula, which is concordant with other species (as aforementioned); however the mouse data did not show this finding in the majority of the brains investigated (the connection was apparent in 4/10 brains bilaterally and hence the data was not presented). The lack of a finding in the mouse likely reflects large robust tracts adjacent to the MGN/S (e.g. internal capsule), dominating the majority of the tractography results and mitigating other projections to cortical areas. It is worth noting here that the general connectivity results show that areas like the auditory cortex, insula, and amygdala required a low threshold to observe in both humans and mice. This reflects that while improvements in the probabilistic algorithm like distance correction and crossing fibers analysis have helped to increase the ability to find tracts, these tracts still are ultimately less common with respect to the major pathways.

There is significant evidence presented here for the convergence of probabilistic tractography and the anterograde tracing findings. While previous work has identified a few points of specific corroboration between anterograde tracing and probabilistic tractography (Gutman et al., 2012), here we provide a more comprehensive and specific comparison

between the two methods. In our data, probabilistic tractography highlight the major fasciculi that contain the projections from the MGN/S seed including the internal capsule, medial lemniscus, and superior cerebral peduncle. Notably, these same major white matter projections were also noted in the anterograde tracing data. Furthermore, the conjunction of the two techniques reveals that probabilistic tractography was able to pick up fibers passing through large portions of the midbrain, thalamus and hypothalamus, which are heterogeneous mixtures of white and grey matter. Since the size of axons is orders of magnitude smaller than the voxel size, it does increase the chances of a false positive or false negative in these areas of heterogenous white and grey matter. This is exhibited in Figure 3 which shows diffuse projections throughout the thalamus, hypothalamus and midbrain. While this can be partially ameliorated with higher and higher thresholds, such thresholding also increases the chances for false positives (e.g. like the auditory cortex in Figure 4). Further, it should be noted, that as seen in Figure 4 and 8, there are actually extensive anterograde projections and terminations throughout the thalamus and hypothalamus (these results are also seen Paul Allen mouse connectivity MG Injections, http://connectivity.brain-map.org/), so diffuse probabilistic results not be immediately discredited. Finally, on this point it should also be considered that the tracing employed in the study was only anterograde, and there are likely extensive projections to the MGN/S that are captured by the probabilistic tractography but not our anterograde tracing.

In terms of study limitations there are few notable points that need addressed with regards to human participant selection, differences in image acquisition, and finally overall data interpretation limitations. First, the human arm of the study was conducted with all African Americans, mostly with female participants and the average age was older than most imaging studies. Looking at the patterns of the three men versus the ten women in all figures suggest that there is not an obvious gender difference. Likewise, age effects were not readily apparent when looking at connectivity between the participants in their 20s and 50s. With regards to race, there is no evidence readily available suggesting it would affect connectivity, but future studies are encouraged to investigate the question further. With regards to imaging acquisition, it should be remarked that the mouse diffusion weighted volumes were collected *ex vivo* while the human volumes were collected *in vivo*. Our previous work has suggested that the *ex vivo* images reliably recapitulate the results seen with classical tracing (Gutman et al., 2012), as does this current study. Finally, with regards to the analysis, the use of diffusion weighted imaging naturally limits the resolution and hence resolving power of the analysis and is also not predictive of direction (e.g. anterograde vs. retrograde). Therefore, it is not possible to further elucidate which of the MGN or surrounding nuclei are contributing to the different paths of connectivity with our current data sets, however, with a recent surge in small animal imaging there are sequences with increasing resolution that may address these questions in the future(Wu et al., 2013). Additionally, the collection of higher resolution data using conventional imaging requires prohibitively long scan times, though advances are growing in the field to ameliorate some of these concerns(Muller et al., 2012). Looking more broadly, diffusion weighted imaging is used widely to make conclusions concerning human patterns of connectivity and also changes in the diffusion measurements of fractional anisotropy and mean diffusivity.

Understanding what these measurements are showing requires the use of well validated animal models, as in the case of this study.

Overall, the preceding discussion and findings provide a foundation against which to study the role of these conserved but poorly understood patterns of MGN/S connectivity. Given the growing literature that implicates the auditory thalamic nuclei in disorders as diverse as tinnitus and schizophrenia there is a need to study these pathways and their function. Additionally, excellent work has begun to demonstrate the role of mice in understanding stress related brain structure and function (Golub et al., 2011; Grunecker et al., 2013). Our data provide a precedent for the use of tractography in a comparative and translationally meaningful way with a small animal model. These findings provide a foundation for future experimental work examining aberrations in connectivity with experimental small animal genetically tractable models like the mouse.

Supplementary Material

Refer to Web version on PubMed Central for supplementary material.

References

Aldhafeeri FM, Mackenzie I, Kay T, Alghamdi J, Sluming V. Neuroanatomical correlates of tinnitus revealed by cortical thickness analysis and diffusion tensor imaging. Neuroradiology. 2012; 54:883–892. [PubMed: 22614806]

Behrens TE, Berg HJ, Jbabdi S, Rushworth MF, Woolrich MW. Probabilistic diffusion tractography with multiple fibre orientations: What can we gain? Neuroimage. 2007; 34:144–155. [PubMed: 17070705]

Behrens TE, Johansen-Berg H, Woolrich MW, Smith SM, Wheeler-Kingshott CA, Boulby PA, Barker GJ, Sillery EL, Sheehan K, Ciccarelli O, Thompson AJ, Brady JM, Matthews PM. Non-invasive mapping of connections between human thalamus and cortex using diffusion imaging. Nat Neurosci. 2003; 6:750–757. [PubMed: 12808459]

Benevento LA, Fallon JH. The ascending projections of the superior colliculus in the rhesus monkey (Macaca mulatta). J Comp Neurol. 1975; 160:339–361. [PubMed: 1112928]

Blum PS, Abraham LD, Gilman S. Vestibular, auditory, and somatic input to the posterior thalamus of the cat. Exp Brain Res. 1979; 34:1–9. [PubMed: 759217]

Brainard MS, Doupe AJ. Interruption of a basal ganglia-forebrain circuit prevents plasticity of learned vocalizations. Nature. 2000; 404:762–766. [PubMed: 10783889]

Brinkhus HB, Carstens E, Zimmermann M. Encoding of graded noxious skin heating by neurons in posterior thalamus and adjacent areas in the cat. Neurosci Lett. 1979; 15:37–42. [PubMed: 530514]

Budinger E, Heil P, Scheich H. Functional organization of auditory cortex in the Mongolian gerbil (Meriones unguiculatus). IV. Connections with anatomically characterized subcortical structures. Eur J Neurosci. 2000; 12:2452–2474. [PubMed: 10947822]

Campeau S, Akil H, Watson SJ. Lesions of the medial geniculate nuclei specifically block corticosterone release and induction of c-fos mRNA in the forebrain associated with audiogenic stress in rats. J Neurosci. 1997; 17:5979–5992. [PubMed: 9221794]

Carlson BA. Diversity matters: the importance of comparative studies and the potential for synergy between neuroscience and evolutionary biology. Arch Neurol. 2012; 69:987–993. [PubMed: 22473771]

Carstens E, Yokota T. Viscerosomatic convergence and responses to intestinal distension of neurons at the junction of midbrain and posterior thalamus in the cat. Exp Neurol. 1980; 70:392–402. [PubMed: 7428903]

Carter DA, Fibiger HC. Ascending projections of presumed dopamine-containing neurons in the ventral tegmentum of the rat as demonstrated by horseradish peroxidase. Neuroscience. 1977; 2:569–576. [PubMed: 917282]

Clasca F, Llamas A, Reinoso-Suarez F. Insular cortex and neighboring fields in the cat: a redefinition based on cortical microarchitecture and connections with the thalamus. J Comp Neurol. 1997; 384:456–482. [PubMed: 9254039]

Clugnet MC, LeDoux JE, Morrison SF. Unit responses evoked in the amygdala and striatum by electrical stimulation of the medial geniculate body. J Neurosci. 1990; 10:1055–1061. [PubMed: 2329366]

Cranford JL, Ladner SJ, Campbell CB, Neff WD. Efferent projections of the insular and temporal neocortex of the cat. Brain Res. 1976; 117:195–210. [PubMed: 990914]

Crippa A, Lanting CP, van Dijk P, Roerdink JB. A diffusion tensor imaging study on the auditory system and tinnitus. Open Neuroimag J. 2010; 4:16–25. [PubMed: 20922048]

Devlin JT, Sillery EL, Hall DA, Hobden P, Behrens TE, Nunes RG, Clare S, Matthews PM, Moore DR, Johansen-Berg H. Reliable identification of the auditory thalamus using multi-modal structural analyses. Neuroimage. 2006; 30:1112–1120. [PubMed: 16473021]

Diedrichsen J, Balsters JH, Flavell J, Cussans E, Ramnani N. A probabilistic MR atlas of the human cerebellum. Neuroimage. 2009; 46:39–46. [PubMed: 19457380]

Diedrichsen J, Maderwald S, Kuper M, Thurling M, Rabe K, Gizewski ER, Ladd ME, Timmann D. Imaging the deep cerebellar nuclei: a probabilistic atlas and normalization procedure. Neuroimage. 2011; 54:1786–1794. [PubMed: 20965257]

Dorph-Petersen KA, Caric D, Saghafi R, Zhang W, Sampson AR, Lewis DA. Volume and neuron number of the lateral geniculate nucleus in schizophrenia and mood disorders. Acta Neuropathol. 2009; 117:369–384. [PubMed: 18642008]

Fani N, Gutman D, Tone EB, Almli L, Mercer KB, Davis J, Glover E, Jovanovic T, Bradley B, Dinov ID, Zamanyan A, Toga AW, Binder EB, Ressler KJ. FKBP5 and attention bias for threat: associations with hippocampal function and shape. JAMA Psychiatry. 2013; 70:392–400. [PubMed: 23407841]

Fani N, King TZ, Jovanovic T, Glover EM, Bradley B, Choi K, Ely T, Gutman DA, Ressler KJ. White matter integrity in highly traumatized adults with and without post-traumatic stress disorder. Neuropsychopharmacology. 2012; 37:2740–2746. [PubMed: 22871912]

Freeman ED, Ipser A, Palmbaha A, Paunoiu D, Brown P, Lambert C, Leff A, Driver J. Sight and sound out of synch: Fragmentation and renormalisation of audiovisual integration and subjective timing. Cortex. 2013

Geiser E, Notter M, Gabrieli JD. A corticostriatal neural system enhances auditory perception through temporal context processing. J Neurosci. 2012; 32:6177–6182. [PubMed: 22553024]

Golub Y, Kaltwasser SF, Mauch CP, Herrmann L, Schmidt U, Holsboer F, Czisch M, Wotjak CT. Reduced hippocampus volume in the mouse model of Posttraumatic Stress Disorder. J Psychiatr Res. 2011; 45:650–659. [PubMed: 21106206]

Grabner G, Janke AL, Budge MM, Smith D, Pruessner J, Collins DL. Symmetric atlasing and model based segmentation: an application to the hippocampus in older adults. Med Image Comput Comput Assist Interv. 2006; 9:58–66. [PubMed: 17354756]

Grahn JA, Brett M. Rhythm and beat perception in motor areas of the brain. J Cogn Neurosci. 2007; 19:893–906. [PubMed: 17488212]

Grunecker B, Kaltwasser SF, Zappe AC, Bedenk BT, Bicker Y, Spoormaker VI, Wotjak CT, Czisch M. Regional specificity of manganese accumulation and clearance in the mouse brain: implications for manganese-enhanced MRI. NMR Biomed. 2013; 26:542–556. [PubMed: 23168745]

Guldin WO, Markowitsch HJ. Cortical and thalamic afferent connections of the insular and adjacent cortex of the cat. J Comp Neurol. 1984; 229:393–418. [PubMed: 6209304]

Gutman DA, Keifer OP Jr, Magnuson ME, Choi DC, Majeed W, Keilholz S, Ressler KJ. A DTI tractography analysis of infralimbic and prelimbic connectivity in the mouse using high-throughput MRI. Neuroimage. 2012; 63:800–811. [PubMed: 22796992]

Gutman DA, Magnuson M, Majeed W, Keifer OP Jr, Davis M, Ressler KJ, Keilholz S. Mapping of the mouse olfactory system with manganese-enhanced magnetic resonance imaging and diffusion tensor imaging. Brain Struct Funct. 2013; 218:527–537. [PubMed: 22527121]

Hart H, Radua J, Nakao T, Mataix-Cols D, Rubia K. Meta-analysis of functional magnetic resonance imaging studies of inhibition and attention in attention-deficit/hyperactivity disorder: exploring task-specific, stimulant medication, and age effects. JAMA Psychiatry. 2013; 70:185–198. [PubMed: 23247506]

Hecht EE, Gutman DA, Preuss TM, Sanchez MM, Parr LA, Rilling JK. Process versus product in social learning: comparative diffusion tensor imaging of neural systems for action execution-observation matching in macaques, chimpanzees, and humans. Cereb Cortex. 2013; 23:1014–1024. [PubMed: 22539611]

Hessler NA, Doupe AJ. Singing-related neural activity in a dorsal forebrain-basal ganglia circuit of adult zebra finches. J Neurosci. 1999; 19:10461–10481. [PubMed: 10575043]

Horie M, Tsukano H, Hishida R, Takebayashi H, Shibuki K. Dual compartments of the ventral division of the medial geniculate body projecting to the core region of the auditory cortex in C57BL/6 mice. Neurosci Res. 2013

Iwata J, LeDoux JE, Meeley MP, Arneric S, Reis DJ. Intrinsic neurons in the amygdaloid field projected to by the medial geniculate body mediate emotional responses conditioned to acoustic stimuli. Brain Res. 1986; 383:195–214. [PubMed: 3768689]

Javad F, Warren JD, Micallef C, Thornton JS, Golay X, Yousry T, Mancini L. Auditory tracts identified with combined fMRI and diffusion tractography. Neuroimage. 2013

Jones, EG. Comparative Anatomy of the Thalamus. In: Jones, EG., editor. The Thalamus. Springer US, Plenum Press; New York: 1985.

Landgrebe M, Langguth B, Rosengarth K, Braun S, Koch A, Kleinjung T, May A, de Ridder D, Hajak G. Structural brain changes in tinnitus: grey matter decrease in auditory and non-auditory brain areas. Neuroimage. 2009; 46:213–218. [PubMed: 19413945]

LeDoux JE, Ruggiero DA, Reis DJ. Projections to the subcortical forebrain from anatomically defined regions of the medial geniculate body in the rat. J Comp Neurol. 1985a; 242:182–213. [PubMed: 4086664]

LeDoux JE, Sakaguchi A, Iwata J, Reis DJ. Auditory emotional memories: establishment by projections from the medial geniculate nucleus to the posterior neostriatum and/or dorsal amygdala. Ann N Y Acad Sci. 1985b; 444:463–464. [PubMed: 3860099]

LeDoux JE, Sakaguchi A, Iwata J, Reis DJ. Interruption of projections from the medial geniculate body to an archi-neostriatal field disrupts the classical conditioning of emotional responses to acoustic stimuli. Neuroscience. 1986; 17:615–627. [PubMed: 3703252]

LeDoux JE, Sakaguchi A, Reis DJ. Subcortical efferent projections of the medial geniculate nucleus mediate emotional responses conditioned to acoustic stimuli. J Neurosci. 1984; 4:683–698. [PubMed: 6707732]

Lein ES, Hawrylycz MJ, Ao N, Ayres M, Bensinger A, Bernard A, Boe AF, Boguski MS, Brockway KS, Byrnes EJ, Chen L, Chen L, Chen TM, Chin MC, Chong J, Crook BE, Czaplinska A, Dang CN, Datta S, Dee NR, Desaki AL, Desta T, Diep E, Dolbeare TA, Donelan MJ, Dong HW, Dougherty JG, Duncan BJ, Ebbert AJ, Eichele G, Estin LK, Faber C, Facer BA, Fields R, Fischer SR, Fliss TP, Frensley C, Gates SN, Glattfelder KJ, Halverson KR, Hart MR, Hohmann JG, Howell MP, Jeung DP, Johnson RA, Karr PT, Kawal R, Kidney JM, Knapik RH, Kuan CL, Lake JH, Laramee AR, Larsen KD, Lau C, Lemon TA, Liang AJ, Liu Y, Luong LT, Michaels J, Morgan JJ, Morgan RJ, Mortrud MT, Mosqueda NF, Ng LL, Ng R, Orta GJ, Overly CC, Pak TH, Parry SE, Pathak SD, Pearson OC, Puchalski RB, Riley ZL, Rockett HR, Rowland SA, Royall JJ, Ruiz MJ, Sarno NR, Schaffnit K, Shapovalova NV, Sivisay T, Slaughterbeck CR, Smith SC, Smith KA, Smith BI, Sodt AJ, Stewart NN, Stumpf KR, Sunkin SM, Sutram M, Tam A, Teemer CD, Thaller C, Thompson CL, Varnam LR, Visel A, Whitlock RM, Wohnoutka PE, Wolkey CK, Wong VY, Wood M, Yaylaoglu MB, Young RC, Youngstrom BL, Yuan XF, Zhang B, Zwingman TA, Jones AR. Genome-wide atlas of gene expression in the adult mouse brain. Nature. 2007; 445:168–176. [PubMed: 17151600]

Lieberman P, Friedman J, Feldman LS. Syntax comprehension deficits in Parkinson's disease. J Nerv Ment Dis. 1990; 178:360–365. [PubMed: 2348189]

Linke R, Schwegler H. Convergent and complementary projections of the caudal paralaminar thalamic nuclei to rat temporal and insular cortex. Cereb Cortex. 2000; 10:753–771. [PubMed: 10920048]

Llano DA, Sherman SM. Evidence for nonreciprocal organization of the mouse auditory thalamocortical-corticothalamic projection systems. J Comp Neurol. 2008; 507:1209–1227. [PubMed: 18181153]

Love JA, Scott JW. Some response characteristics of cells of the magnocellular division of the medial geniculate body of the cat. Can J Physiol Pharmacol. 1969; 47:881–888. [PubMed: 5346442]

Mai, JK.; Paxinos, G.; Voss, T. Atlas of the human brain. Academic Press; New York; London: 2008. p. viii271 p. ill. (some col.) 236 cm. + 271 DVD-ROM (274 273/274 in)

Manger PR, Cort J, Ebrahim N, Goodman A, Henning J, Karolia M, Rodrigues SL, Strkalj G. Is 21st century neuroscience too focussed on the rat/mouse model of brain function and dysfunction? Front Neuroanat. 2008; 2:5. [PubMed: 19127284]

McGeorge AJ, Faull RL. The organization of the projection from the cerebral cortex to the striatum in the rat. Neuroscience. 1989; 29:503–537. [PubMed: 2472578]

Mesulam MM, Pandya DN. The projections of the medial geniculate complex within the sylvian fissure of the rhesus monkey. Brain Res. 1973; 60:315–333. [PubMed: 4202852]

Monakow, Cv. Die Lokalisation im Grosshirn und der Abbau der Funktion durch kortikale Herde. Wiesbaden, S., editor. 1914. p. 800

Moriizumi T, Hattori T. Ultrastructural morphology of projections from the medial geniculate nucleus and its adjacent region to the basal ganglia. Brain Res Bull. 1992; 29:193–198. [PubMed: 1381984]

Muhlau M, Rauschecker JP, Oestreicher E, Gaser C, Rottinger M, Wohlschlager AM, Simon F, Etgen T, Conrad B, Sander D. Structural brain changes in tinnitus. Cereb Cortex. 2006; 16:1283–1288. [PubMed: 16280464]

Muller HP, Vernikouskaya I, Ludolph AC, Kassubek J, Rasche V. Fast diffusion tensor magnetic resonance imaging of the mouse brain at ultrahigh-field: aiming at cohort studies. PLoS One. 2012; 7:e53389. [PubMed: 23285289]

Ottersen OP, Ben-Ari Y. Afferent connections to the amygdaloid complex of the rat and cat. I. Projections from the thalamus. J Comp Neurol. 1979; 187:401–424. [PubMed: 489786]

Poliak S. Untersuchungen am Octavus-system der Saugetiere und an den mit diesen koordinierten motorischen Apparaten des Hirnstamms. Journal für Psychologie und Neurologie. 1926; 32:S.170.

Power BD, Kolmac CI, Mitrofanis J. Evidence for a large projection from the zona incerta to the dorsal thalamus. J Comp Neurol. 1999; 404:554–565. [PubMed: 9987997]

Preuss TM. Taking the measure of diversity: comparative alternatives to the model-animal paradigm in cortical neuroscience. Brain Behav Evol. 2000; 55:287–299. [PubMed: 10971014]

Raffaele R, Sapienza S, Urbano A. Fastigial nucleus projections in the pars magnocellularis of the medial geniculate body of the cat. Boll Soc Ital Biol Sper. 1969; 45:1296–1298. [PubMed: 5386568]

Redies H, Brandner S, Creutzfeldt OD. Anatomy of the auditory thalamocortical system of the guinea pig. J Comp Neurol. 1989; 282:489–511. [PubMed: 2723149]

Rilling JK, Glasser MF, Preuss TM, Ma X, Zhao T, Hu X, Behrens TE. The evolution of the arcuate fasciculus revealed with comparative DTI. Nat Neurosci. 2008; 11:426–428. [PubMed: 18344993]

Roger M, Arnault P. Anatomical study of the connections of the primary auditory area in the rat. J Comp Neurol. 1989; 287:339–356. [PubMed: 2778109]

Ryugo DK, Killackey HP. Differential telencephalic projections of the medial and ventral divisions of the medial geniculate body of the rat. Brain Res. 1974; 82:173–177. [PubMed: 4611594]

Schweitzer JB, Lee DO, Hanford RB, Zink CF, Ely TD, Tagamets MA, Hoffman JM, Grafton ST, Kilts CD. Effect of methylphenidate on executive functioning in adults with attention-deficit/hyperactivity disorder: normalization of behavior but not related brain activity. Biol Psychiatry. 2004; 56:597–606. [PubMed: 15476690]

Shammah-Lagnado SJ, Alheid GF, Heimer L. Efferent connections of the caudal part of the globus pallidus in the rat. J Comp Neurol. 1996; 376:489–507. [PubMed: 8956113]

Shinonaga Y, Takada M, Mizuno N. Direct projections from the non-laminated divisions of the medial geniculate nucleus to the temporal polar cortex and amygdala in the cat. J Comp Neurol. 1994; 340:405–426. [PubMed: 8188859]

Smith MJ, Wang L, Cronenwett W, Mamah D, Barch DM, Csernansky JG. Thalamic morphology in schizophrenia and schizoaffective disorder. J Psychiatr Res. 2011; 45:378–385. [PubMed: 20797731]

Smith SM. Fast robust automated brain extraction. Hum Brain Mapp. 2002; 17:143–155. [PubMed: 12391568]

Smulders TV. The relevance of brain evolution for the biomedical sciences. Biol Lett. 2009; 5:138–140. [PubMed: 18940773]

Su YY, Luo B, Jin Y, Wu SH, Lobarinas E, Salvi RJ, Chen L. Altered neuronal intrinsic properties and reduced synaptic transmission of the rat's medial geniculate body in salicylate-induced tinnitus. PLoS One. 2012; 7:e46969. [PubMed: 23071681]

Thiebaut de Schotten M, Dell'Acqua F, Valabregue R, Catani M. Monkey to human comparative anatomy of the frontal lobe association tracts. Cortex. 2012; 48:82–96. [PubMed: 22088488]

Tunturi AR. A study on the pathway from the medial geniculate body to the acoustic cortex in the dog. Am J Physiol. 1946; 147:311–319. [PubMed: 21000753]

Walker AE. The Projection of the Medial Geniculate Body to the Cerebral Cortex in the Macaque Monkey. J Anat. 1937; 71:319–331. [PubMed: 17104643]

Wang J, Palkovits M, Usdin TB, Dobolyi A. Afferent connections of the subparafascicular area in rat. Neuroscience. 2006; 138:197–220. [PubMed: 16361065]

Wepsic JG. Multimodal sensory activation of cells in the magnocellular medial geniculate nucleus. Exp Neurol. 1966; 15:299–318. [PubMed: 5947925]

Winer JA, Diehl JJ, Larue DT. Projections of auditory cortex to the medial geniculate body of the cat. J Comp Neurol. 2001; 430:27–55. [PubMed: 11135244]

Winer JA, Morest DK. The medial division of the medial geniculate body of the cat: implications for thalamic organization. J Neurosci. 1983; 3:2629–2651. [PubMed: 6655503]

Wu D, Xu J, McMahon MT, van Zijl PC, Mori S, Northington FJ, Zhang J. In vivo high-resolution diffusion tensor imaging of the mouse brain. Neuroimage. 2013; 83:18–26. [PubMed: 23769916]

Xia S, Li X, Kimball AE, Kelly MS, Lesser I, Branch C. Thalamic shape and connectivity abnormalities in children with attention-deficit/hyperactivity disorder. Psychiatry Res. 2012; 204:161–167. [PubMed: 23149038]

Zhang D, Guo L, Zhu D, Li K, Li L, Chen H, Zhao Q, Hu X, Liu T. Diffusion tensor imaging reveals evolution of primate brain architectures. Brain Struct Funct. 2012

Zimny R, Sobusiak T, Kotecki A, Deja A. The medial geniculate body afferents from the cerebellum in the rabbit as studied with the method of orthograde degeneration. J Hirnforsch. 1981; 22:573–585. [PubMed: 7328312]

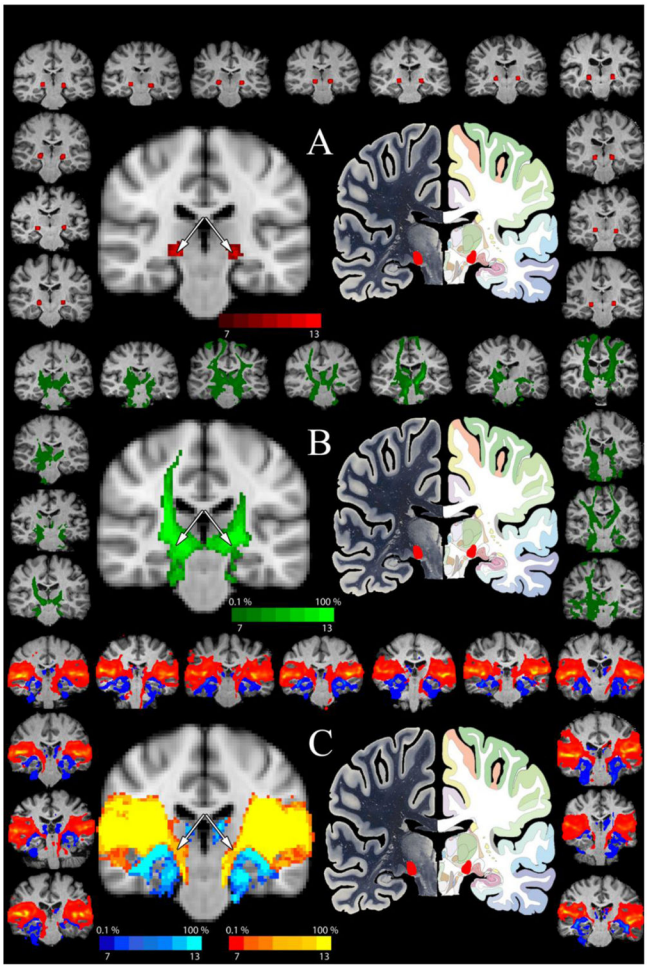

Figure 1. Determination of the Human MGN/S Seed

Panel A shows the summation of the MGN/S seed (red) on a standard MNI template (center left) with the atlas image (central right, www.thehumanbrain.info) provided for comparison. The surrounding brains show the placement of the seed on the T1 anatomical image for each participant individually. Panel B shows the patterns of connectivity (in green) for the inferior colliculus seed. The central left brain shows the summation of all participants in MNI152 space (threshold set 0.1% tracts and to a minimum of 7 of the 13 brains showing the results as indicated on the top of the color key). The perimeter shows the individual IC tractography results for the IC seed thresholded at 0.1%. Looking at the central summation figure, notice the overlap of the inferior colliculus pathways with the placement of the MGN/S seed in Panel A – as indicated by the white arrows. Likewise, panel C shows the same summation map of the probabilistic tractography of the primary visual cortex (dark blue to bright blue) and the summation map of the projections of the primary auditory cortex (red to yellow). In the central summation figure, notice the overlap of the auditory pathways with the placement of the MGN/S seed in Panel A – as indicated by the white arrows.

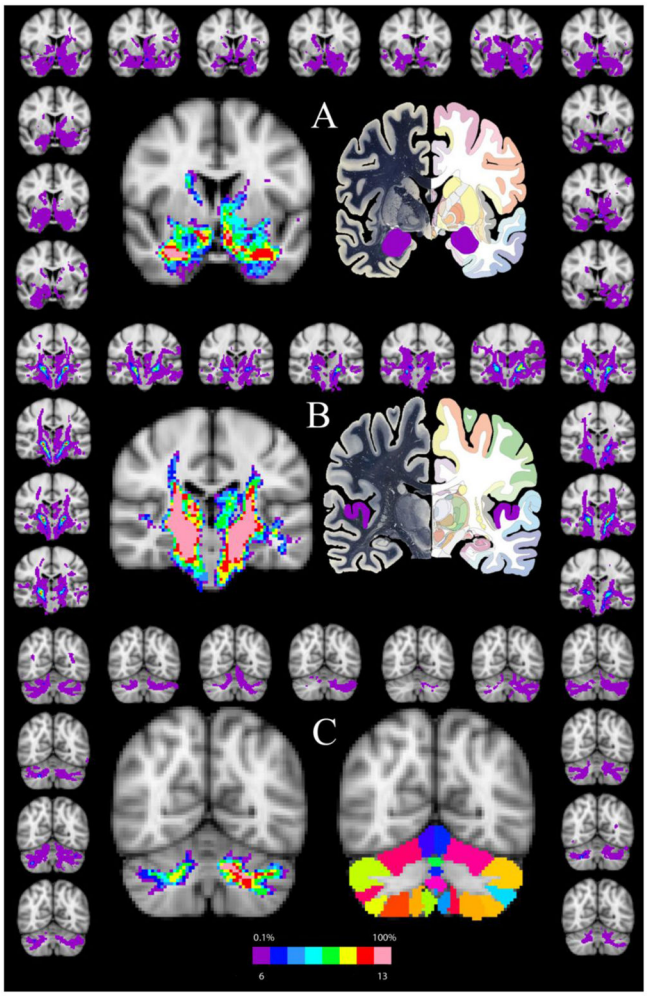

Figure 2. The Probabilistic Connections of the Human MGN/S

Panel A shows the general pattern of connectivity between the MGN/S and the amygdala (highlighted on the Human Brain Atlas image in purple) and also portions of the caudate, putamen, and globus pallidus. As in Figure 1, the left central figure is the summation of the binarized tracts from all subjects overlaid onto the MNI152 brain (threshold set at 0.1% tracts and 6 of the 13 participants showing the connectivity). The surrounding brains are the individual results (matched in position to Figure 1) thresholded a 0.1%. Panel B is analogous in layout to Panel A and shows the connectivity of the medial geniculate to the thalamus, auditory cortex, middle temporal cortex, insula, and portions of the midbrain. Likewise, Panel C shows the connectivity of MGN/S and cerebellum, with the right central image representing the probabilistic cerebellar atlas included with FSL.

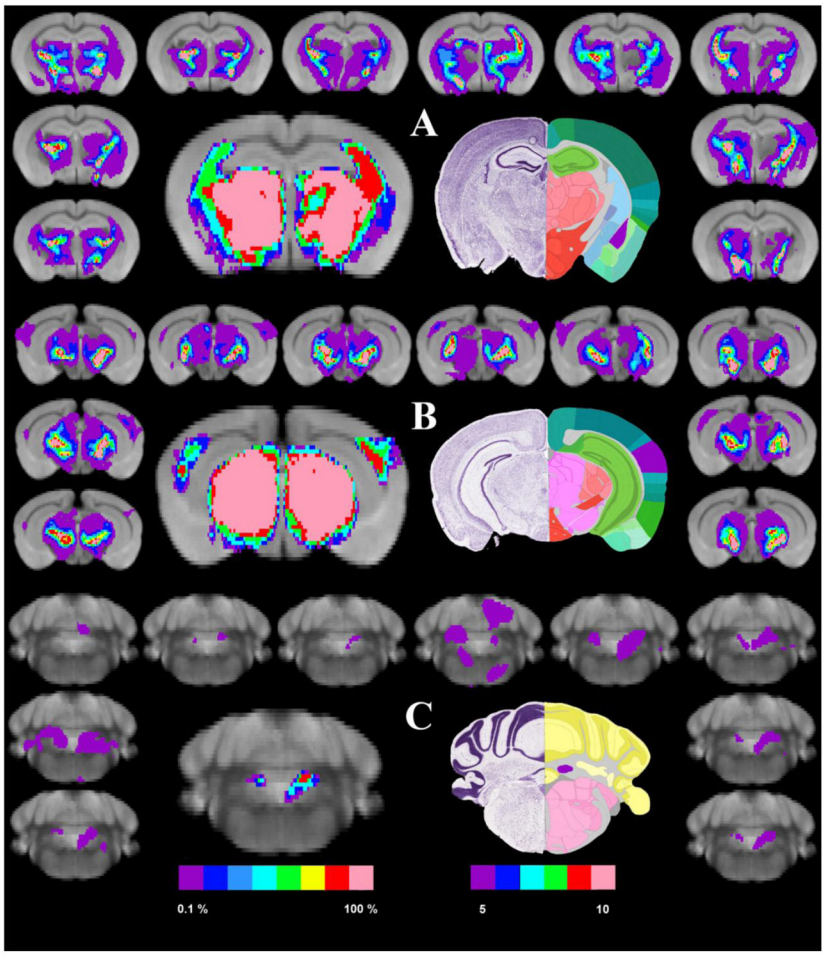

Figure 3. The Probabilistic Connections of the Mouse Medial Geniculate Nucleus

Panel A shows the connectivity of the MGN/S and the caudate/putamen (light blue) and the amygdala (highlighted in purple, along with the thalamus and hypothalamus. Following the layout of the previous figures, the left central figure is the summation of the thresholded and binarized probabilistic tractography results from all participants overlaid onto our standard 24 average mouse brain (5 of 10 mice showing the connectivity). The surrounding smaller brains are the individual probabilistic tractography results overlaid onto the standard mouse brain. The right central figure is the closest corresponding section from the Paul Allen brain atlas. Panel B shows the connectivity of the medial geniculate and the thalamus, hypothalamus, auditory cortex, and portions of the midbrain and spinal tracts. Panel C shows the connectivity of MGN/S and cerebellum.

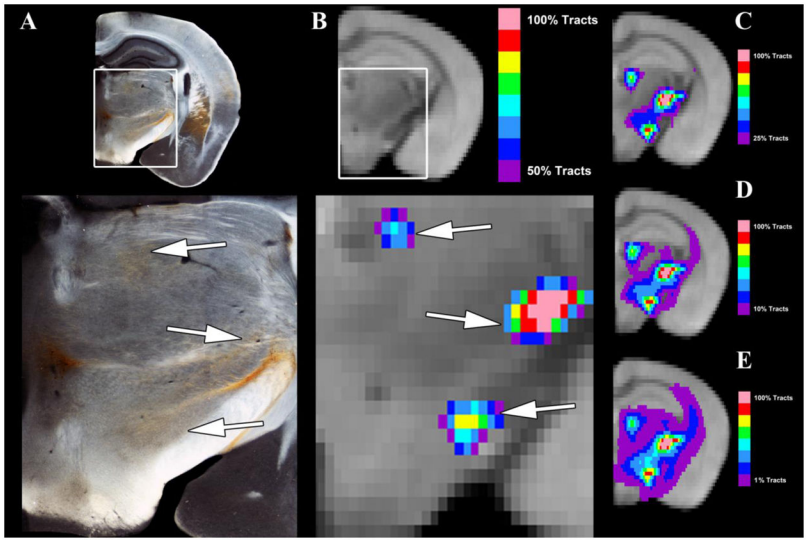

Figure 4. A Focused Comparison of Anterograde Tracing and Probabilistic Tractography in the Midbrain and Thalamus

Panel A shows the BDA anterograde tracing results for injections into the MGN/S, with notable pathways to the hypothalamus (zona incerta and lateral hypothalamus) and thalamus (lateral posterior and central median nucleus). Panel B shows an extensively thresholded (50% of tracts) average tractography results, which corresponds to the Panel A, that accurately correspond to those in Panel A (indicated with white arrows). Panel C–E shows the same average probabilistic tractography, though with different threshold values. Note that Panel A has rather diffuse tracts running across the thalamus and hypothalamus, which are most closely recapitulated in Panel E with the 1% threshold. Yet even at the 1% threshold there is a loss of the auditory cortex connections that are apparent at 0.1% thresholding in Figure 4B.

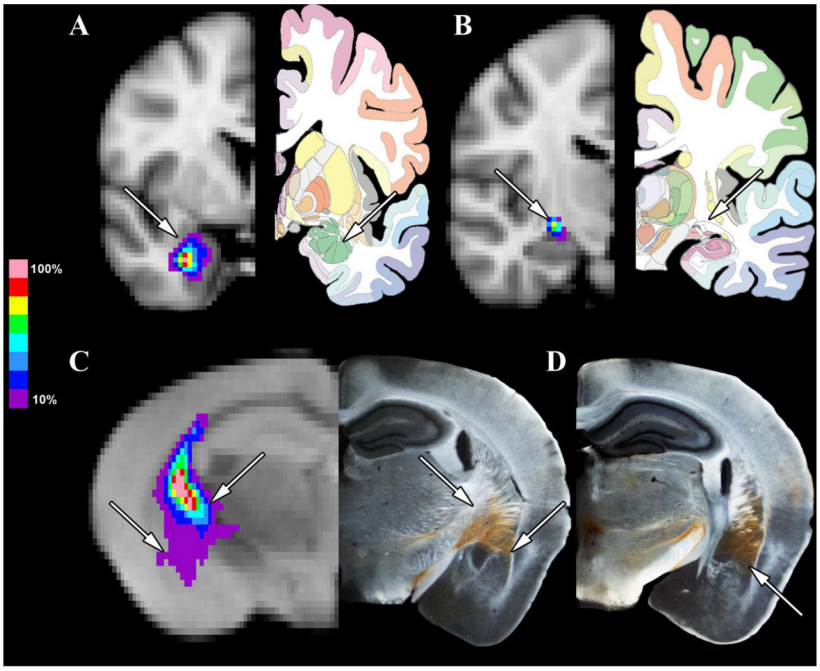

Figure 5. A Focused Comparison of Human and Mouse MGN/S and the Amygdala

Panel A shows the average probabilistic tractography (thresholded at 10%) between the human MGN/S and amygdala (the amygdala is indicated by the white arrow). Panel B shows a section posterior to Panel A to highlight that the pathway between the MGN/S and amygdala is the internal capsule (indicated by the arrow). In parallel, Panel C the average probabilistic tractography results (thresholded at 10%) between the mouse MGN/S and the amygdala, along with the concordance to the anterograde tracing results (lateral white arrows point out the amygdala, medial white arrows point out the fibers of passage through the internal capsule). Panel D shows the more extensive amygdala connections in an adjacent posterior section.

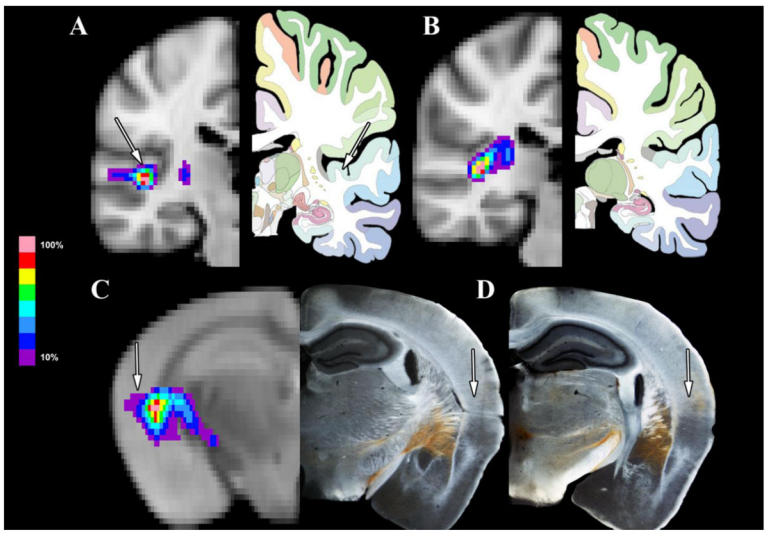

Figure 6. A Focused Comparison of Human and Mouse MGN/S and Auditory Cortex Connectivity

Panel A shows the average probabilistic tractography (thresholded at 10%) between the human MGN/S and Auditory Cortex (the auditory cortex is indicated by the white arrow). Panel B shows a section posterior to Panel A to highlight that the pathway between the MGN/S and auditory cortex is the internal capsule. In parallel, Panel C the average probabilistic tractography results between the mouse MGN/S and the auditory cortex, along with the concordance to the anterograde tracing results (white arrows point out the auditory cortex. Panel D shows the more extensive auditory cortex connections in an adjacent posterior section (indicated by white arrow).

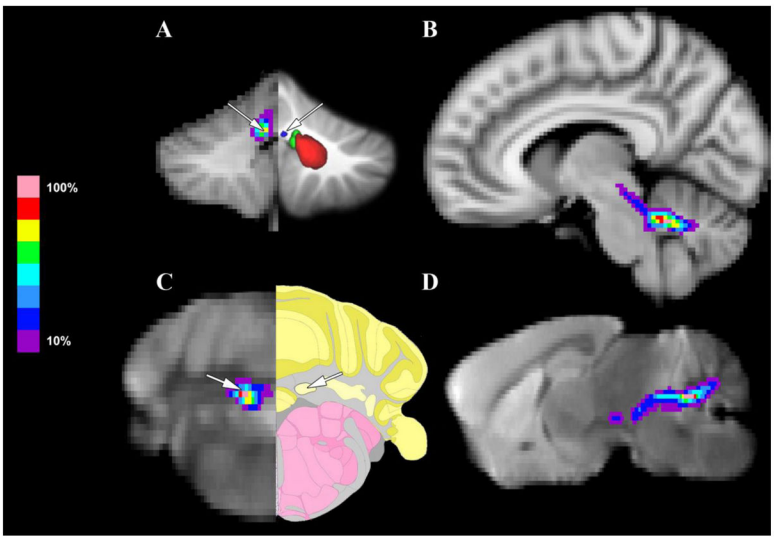

Figure 7. A Focused Comparison of Human and Mouse MGN/S and Fastigial Nucleus of the Cerebellum Connectivity

Panel A shows the average probabilistic tractography (thresholded at 10%) between the human MGN/S and cerebellum (the fastigial nucleus is indicated by the white arrow, as compared to a previously published atlas of the cerebellum). Panel B shows a sagittal section that highlights that the pathway between the MGN/S and fastigial nucleus of the cerebellum is the superior cerebellar peduncle. In parallel, Panel C the average probabilistic tractography results between the mouse MGN/S and the fastigial nucleus of the cerebellum (indicated by the white arrow on the tractography and Paul Allen mouse brain atlas). Panel D shows a sagittal section that highlights the pathway of the connectivity between the fastigial nucleus and the MGN/S which is the superior cerebellar peduncle.

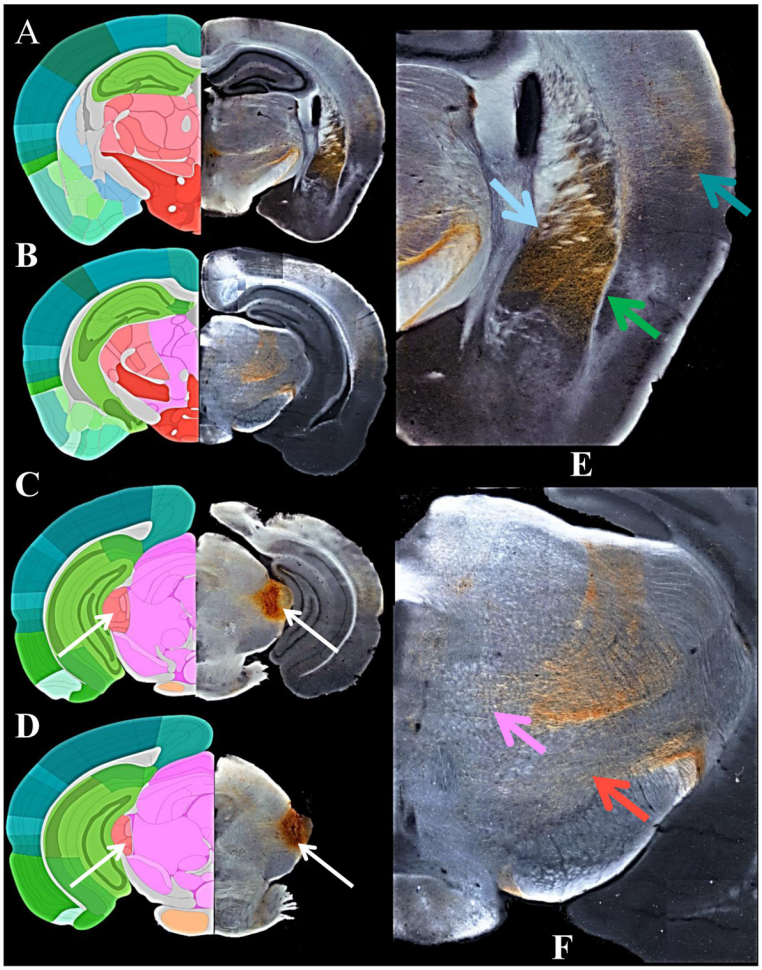

Figure 8. The Anterograde Classical Tracing Results of the MGN/S

The whole brain sections on the left (Panels A–D, Sections 75,) are a composite of the most representative slice from one mouse. Panel A shows the extensive **amygdala, auditory cortex,** and **caudate-putamen** projections which course through the internal capsule. Panels B and C show that there are also notable projections and fibers of passage in the **hypothalamus**, **thalamus,** and **midbrain.** Panels C and D show that the injection site the predominantly resides in the MGN/S (as indicated by the white arrows). The right two sections (E & F) are magnifications of the **amygdala,/ caudate-putamen** plus **auditory cortex** on top from the upper left section and the magnification of the high density of fibers of termination and passage through the **thalamus**, **hypothalamus**, and **midbrain** from the upper middle section. Note that there are more subtle tracts present throughout the thalamus, hypothalamus, and midbrain that are not apparent on the image reproduction, even Panels E and F.

Table 1

Comparison of the Human Probabilistic Tractography and Mouse Anterograde and Probabilistic Tractography as Seeded in the MGN/S

Brain Area with MGN/S Connectivity	General Human Probabilistic Tractography		General Mouse Probabilistic Tractography		Mouse BDA Case Study Anterograde Tracing
Hemisphere	**Left**	**Right**	**Left**	**Right**	Right
Auditory Cortex[*]	8 of 13	8 of 13	9 of 10	9 of 10	Very Dense
Insular Cortex	13 of 13	13 of 13	4 of 10 (not shown)	4 of 10 (not shown)	Very Sparse
Amygdala Complex[†]	12 of 13	13 of 13	6 of 10	6 of 10	Central, Medial, Lateral Nuclei
Pallidum	13 of 13	13 of 13	7 of 10	6 of 10	Substantia Innomiata, Globus Pallidus
Caudate Putamen[‡]	13 of 13	13 of 13	10 of 10	10 of 10	Very Dense
Thalamus	13 of 13	13 of 13	10 of 10	10 of 10	Lateral Posterior, Subparafasicular, Interomedial Dorsal, and Ventral Posterior areas/nuclei and Posterior Complex
Hypothalamus	13 of 13	13 of 13	10 of 10	10 of 10	Anterior Hypothalamic Nucleus, Subparaventricular Zone, Peri and Paraventricular Nuclei, Zona Incerta, Subthalamic nucleus
Pons	13 of 13	13 of 13	10 of 10	10 of 10	Pontine grey
Midbrain[~]	13 of 13	13 of 13	10 of 10	10 of 10	Periaqueductal grey and Superior/inferior colliculus
Cerebellum[•]	13 of 13	11 of 13	10 of 10	9 of 10	Not Observed

[*] see Figure 6 for a focused probabilistic tractography analysis

[†] see Figure 5 for a focused probabilistic tractography analysis

[‡] see Figures 3, 4,5

[•] see Figure 4 for a focused probabilistic tractography analysis,

[~] see Supplemental Figure 1 for a focused probabilistic tractography analysis,

[°] see Figure 7 for a focused probabilistic tractography analysis